Title: Exposure duration modulates the response of Caribbean corals to global change stressors

Running Title: Exposure duration modulates coral physiology

List of Authors: Aichelman HE[1,2], Bove CB[3], Castillo KD[2,3], Boulton JM[2], Knowlton AC[2], Nieves OC[1], Ries JB[4], Davies SW[1,2,4]

Institutional Affiliations
[1]Department of Biology, Boston University, Boston, MA, USA
[2]Department of Marine Sciences, University of North Carolina at Chapel Hill, Chapel Hill, NC, USA
[3]Environment, Ecology, and Energy Program, University of North Carolina at Chapel Hill, Chapel Hill, NC, USA
[4]Department of Marine and Environmental Sciences, Northeastern University, Boston, MA, USA

Contact Information: hannahaichelman@gmail.com; (704) 607-7408

Abstract

Global change is threatening coral reefs, with rising temperatures leading to repeat bleaching events (dysbiosis of coral hosts and their symbiotic algae) and ocean acidification reducing net coral calcification. Although global-scale mass bleaching events are revealing fine-scale patterns of coral resistance and resilience, traits that lead to persistence under environmental stress remain elusive. Here, we conducted a 95-day controlled-laboratory experiment to investigate how duration of exposure to ocean warming (28, 31°C), acidification (pCO_2 = 400–2800 µatm), and their interaction influence the physiological responses of two Caribbean reef-building coral species (*Siderastrea siderea*, *Pseudodiploria strigosa*) from two reef zones of the Belize Mesoamerican Barrier Reef System. Every 30 days, calcification rate, total host protein and carbohydrate, chlorophyll *a* pigment concentration, and symbiont cell density were quantified for the same coral colony to characterize acclimatory responses of each genotype. Physiologies of the two species were differentially affected by these stressors, with exposure duration modulating responses. *Siderastrea siderea* was most affected by extreme pCO_2 (~2800 µatm), which resulted in reduced calcification rate, symbiont density, and chlorophyll *a* concentration. *Siderastrea siderea* calcification rate initially declined under extreme pCO_2 but recovered by the final time point, and overall demonstrated resistance to next-century pCO_2 and temperature stress. In contrast, *P. strigosa* was more negatively impacted by elevated temperature (31°C). Reductions in *P. strigosa* calcification rate and total carbohydrates were consistently observed over time regardless of pCO_2 treatment, with the greatest reductions observed under elevated temperature. However, nearshore colonies of *P. strigosa* maintained calcification rates under elevated temperature throughout all exposure durations, suggesting individuals from this environment may be locally adapted to the warmer temperatures characterizing their natal reef zone. This experiment highlights how tracking individual coral colony physiology across broad exposure durations can capture acclimatory responses of corals to global change stressors.

Keywords: coral physiology, temperature stress, ocean acidification, *Siderastrea siderea*, *Pseudodiploria strigosa*

1. Introduction

Since the Industrial Revolution, anthropogenic activities have increased the partial pressure of atmospheric carbon dioxide (pCO_2), which has warmed the atmosphere by approximately 0.6°C (Pörtner et al., 2019). As atmospheric temperatures increase, so do sea surface temperatures (SSTs), a trend that has continued since 1970 (Pörtner et al., 2019). Increasing atmospheric pCO_2 has also caused surface ocean pH to decrease at a rate of 0.017 to 0.027 units per decade since the 1980s, potentially exacerbating the impacts of warming SSTs on marine organisms (e.g. Pörtner et al., 2019). The resulting warming and acidification have impacted organisms across the globe, as thermal niches shift and habitats rapidly change (Morley et al., 2018; Parmesan and Yohe, 2003; Pörtner et al., 2019). The negative effects of global change are predicted to strengthen and, under the Intergovernmental Panel on Climate Change's (IPCC) most extreme emissions scenario (RCP8.5), oceans are expected to take up 5 to 7 times more heat and decrease by 0.3 pH units by 2100 (Pörtner et al., 2019).

Coral reefs are valuable economic and ecological resources (Costanza et al., 2014) that are particularly vulnerable to ocean warming and acidification. The high biodiversity of coral reefs depends on the obligate symbiosis between the coral animal and its symbiotic algae of the family Symbiodiniaceae (previously genus *Symbiodinium*; LaJeunesse et al., 2018). This symbiosis is sensitive to thermal anomalies and, because tropical coral species live within 1°C of their upper thermal limit, even slight increases in SST can result in bleaching (breakdown of the coral-algal symbiosis) and ultimately mortality if the symbionts fail to repopulate the coral host. Global coral bleaching events are occurring with increasing frequency and severity as SST continues to increase (Hughes et al., 2017).

Ocean acidification is the result of increased atmospheric CO_2 dissolving into seawater, reducing its pH, and altering its carbonate chemistry (Doney et al., 2009; Orr et al., 2005). This

alteration of carbonate chemistry includes a decrease in carbonate ion concentration ([CO_3^{2-}]), which reduces the saturation state of seawater with respect to aragonite (Ω_{arag})—which can make it more challenging for corals to build their aragonite skeletons (Doney et al., 2009; Kleypas et al., 1999). Laboratory experiments have shown that ocean acidification conditions projected for the end of next century can have negative (Comeau et al., 2013; Hoegh-Guldberg et al., 2007; Horvath et al., 2016; Kroeker et al., 2010), neutral (Reynaud et al., 2003; Ries et al., 2010), and parabolic (Castillo et al., 2014) impacts on coral calcification, while field experiments have yielded more negative outcomes (Albright et al., 2018; Comeau et al., 2019; Jokiel et al., 2008; Kline et al., 2019). The direction and magnitude of calcification responses to acidification are influenced by many factors (Kornder et al., 2018), including ability to regulate calcifying fluid chemistry in support of calcification (e.g. Ries, 2011), species differences (Bove et al., 2019; Okazaki et al., 2017), calcification rate under ambient conditions (Shaw et al., 2016), CO_2-induced fertilization of photosynthesis (Castillo et al., 2014), coral gender (Holcomb et al., 2012), experimental duration (Kline et al., 2019), co-occurring thermal stress (Anthony et al., 2011; Kroeker et al., 2013), and heterotrophic capacity (Cohen and Holcomb, 2009; Towle et al., 2015). Coral calcification in response to temperature stress is similarly complicated by a number of factors, and a meta-analysis by Kornder et al. (2018) highlighted strong taxonomic variation and that thermal stress is more pronounced in adults and during the summer. Similar to acidification, coral calcification under elevated temperature can be mediated by heterotrophic capacity (Aichelman et al., 2016; Grottoli et al., 2006; Rodolfo-Metalpa et al., 2008; Towle et al., 2015). In addition to considering calcification rate, energetic reserves are critical to coral health and resistance to stressors, and have been associated with bleaching susceptibility

(Anthony et al., 2009; Grottoli et al., 2014; Levas et al., 2018) and in determining whether a bleaching event will lead to mortality (Anthony et al., 2009; Grottoli et al., 2006).

Fewer studies consider the combined effects of temperature and acidification stress and, similar to studies investigating the effects of independent stressors, such experiments have produced variable results. Several studies have demonstrated that elevated temperatures have stronger negative effects on the coral holobiont (combination of coral animal, algal symbiont, and associated microbiota) when compared to acidification, including negative effects on calcification rates (Anderson et al., 2019; Schoepf et al., 2013), larval development (Chua et al., 2013), and survivorship (Anderson et al., 2019). Although no studies have found synergistic effects of temperature and acidification on coral calcification (i.e. combined effects are greater than sum of individual effects), numerous studies have demonstrated that the effects of temperature and acidification stress can be additive, in terms of impacts on coral calcification (Agostini et al., 2013; Edmunds et al., 2012; Horvath et al., 2016; Kornder et al., 2018; Prada et al., 2017; Rodolfo-Metalpa et al., 2011) and metabolism (Agostini et al., 2013). A more complete understanding of the combined effects of global change stressors will require investigations of multiple species and stressors across longer timescales with a focus on multiple physiology metrics.

The effects of global change on the coral holobiont not only vary by the stressors in question, but also by species. Species differences in response to global change stressors have been observed in coral calcification rate (Bove et al., 2019; Edmunds et al., 2012; Edmunds et al., 2019; Okazaki et al., 2017) and recovery of energetic reserves through time (i.e. total soluble lipid; Levas et al., 2018). Additionally, spatial scale appears to play a role in some corals' responses to global change, with differential stress tolerance observed across populations along a

reef system (e.g. the Great Barrier Reef; Dixon et al., 2015) and across reef zones (Castillo et al., 2012; Kenkel et al., 2013a; Kenkel et al., 2013b; Kenkel and Matz, 2016). Differences in coral thermal tolerance can occur on spatial scales as small as between tidal pools in American Samoa (Bay and Palumbi, 2014; Oliver and Palumbi, 2011; Palumbi et al., 2014), illustrating that adaptation and/or acclimation to fine scale environmental differences can play a role in determining coral response to global change stressors.

In addition to understanding stress responses across species and spatial scales, considering how duration of stress exposure affects the physiological response of the coral holobiont is critical (McLachlan et al., 2020). This goal is complicated by the difficulty of executing long-term laboratory (*ex situ*) experiments, and it is therefore relatively rare for studies to track coral physiology under controlled conditions for extended periods of time. However, several studies have been conducted for approximately 90 days or more (e.g., Anderson et al., 2019; Bove et al., 2019; Castillo et al., 2014; Comeau et al., 2019; Kline et al., 2019), and each reveal nuanced patterns of stress and resilience in corals. For example, Comeau et al. (2019) observed that acidification (1,050 µatm pCO_2) caused a rapid, but species-specific, alteration of calcifying fluid chemistry in four coral and two calcifying algae species throughout the entire one-year duration of the experiment (Comeau et al., 2019). Additionally, by measuring *S. siderea* growth every 30 days throughout a 90-day experiment, Castillo et al. (2014) showed that calcification responses to acidification (604 µatm pCO_2) varied substantially through time—with calcification rates increasing in response to moderate acidification (604 µatm pCO_2) between 0 and 60 days, and decreasing between 60 and 90 days. Finally, Levas et al. (2018) tracked corals for 11 months following experimental bleaching and found interspecific differences in the timing of recovery. Specifically, *Porites divaricata* initially catabolized lipids and decreased

calcification but largely recovered within 11 months, while *P. astreoides* fully recovered within 1.5 months after increasing feeding and symbiont nitrogen uptake (Levas et al., 2018). It is therefore clear that tracking coral physiology through time can provide valuable insights into how corals respond to short-, moderate-, and long-term global change stress.

Here, two ecologically important reef-building coral species (*Siderastrea siderea* and *Pseudodiploria strigosa*) from two reef zones (forereef and nearshore) of the Belize Mesoamerican Barrier Reef System (MBRS) were maintained under a fully crossed acidification (ca. 400 µatm [present day], ca. 640 µatm [next century], ca. 2800 µatm [extreme]) and temperature (28, 31°C) experiment for 95 days. In order to characterize the responses of these species to projected global change, holobiont physiology of each coral colony was monitored every 30 days (exposure duration: 0-30 days = T_0-T_{30} = short-term, 30-60 days = T_{30}-T_{60} = moderate-term, 60-95 days = T_{60}-T_{95} = long-term), including metrics for both the coral host (calcification rate, total protein, total carbohydrates) and symbiont (symbiont cell density, chlorophyll *a* pigment concentration). The work presented here elucidates the impact of exposure duration on corals' acclimatory response to global change stressors.

2. Materials and methods

(2.1) Coral collection and experimental design

Data presented here are from an experiment run in parallel with an experiment published by Bove et al. (2019). Therefore, experimental design and culturing conditions are similar to those presented therein. However, data presented here pertain to a different suite of coral individuals than explored in Bove et al. (2019), and only two species (instead of four) are explored in the present study. Timing of the two experiments is also staggered by 30 days; for

comparison time T_0 in the present experiment corresponds to the "pre-acclimation period" in Bove et al. (2019). Methods specific to this experiment are presented below. However, readers are referred to Bove et al. (2019) for methods that pertain to both studies, such as those relating to the control and monitoring of seawater carbonate chemistry parameters.

Three colonies of *Siderastrea siderea* and *Pseudodiploria strigosa* were collected from a nearshore (NS; Port Honduras Marine Reserve, PHMR; 16°11'23.5314"N, 88°34'21.9360"W) and a forereef (FR; Sapodilla Cayes Marine Reserve, SCMR; 16°07'00.0114"N, 88°15'41.1834"W) site along the southern portion of the Belize Mesoamerican Barrier Reef System (MBRS) in June 2015 (N=3/species/site; Figure 1). Colonies were separated by at least 5 m to maximize the likelihood of obtaining genetically distinct individuals. Following collection, all coral colonies (3 colonies x 2 reef zones x 2 species = 12 putative genotypes) were transported to the Northeastern University (NU) Marine Science Center and fragmented into 24 genetically identical fragments. One FR *P. strigosa* colony did not survive fragmentation, leaving a total of 3 genotypes for NS and FR *S. siderea*, 3 genotypes for NS *P. strigosa*, and 2 genotypes for FR *P. strigosa* genotypes (total of 6 *S. siderea* and 5 *P. strigosa* genotypes). After fragmentation, coral fragments were allowed to recover for 23 days in natural flow-through seawater with salinity and temperature ($\pm$SD) of 30.7$\pm$0.8 and 28.2$\pm$0.5°C, respectively. After recovery, temperature and pCO_2 were incrementally adjusted over a period of 20 days until target treatment conditions were achieved. During this time, temperatures of the elevated temperature treatments were increased by 0.4°C every 3 days and pCO_2 was adjusted by 0 µatm (present day), +30 µatm (end of century), and +240 µatm (extreme) every 3 days. The six experimental treatments consisted of a full factorial design of two temperatures (target 28, 31°C) and three pCO_2 levels (target 400, 700, 2800 µatm). Coral fragments were distributed such that

four replicate fragments from each genotype were represented in each of the six experimental treatments. The six experimental treatments were replicated in three aquaria, for a total of 18 42L acrylic aquaria. Each aquaria was illuminated on a 10:14 h light:dark cycle with 300 µmol photons m^{-2} s^{-1} of photosynthetically active radiation (PAR). The experimental system used natural flow-through seawater and coral fragments were fed every other day with a mixture of frozen adult *Artemia* sp. and freshly hatched *Artemia* sp.

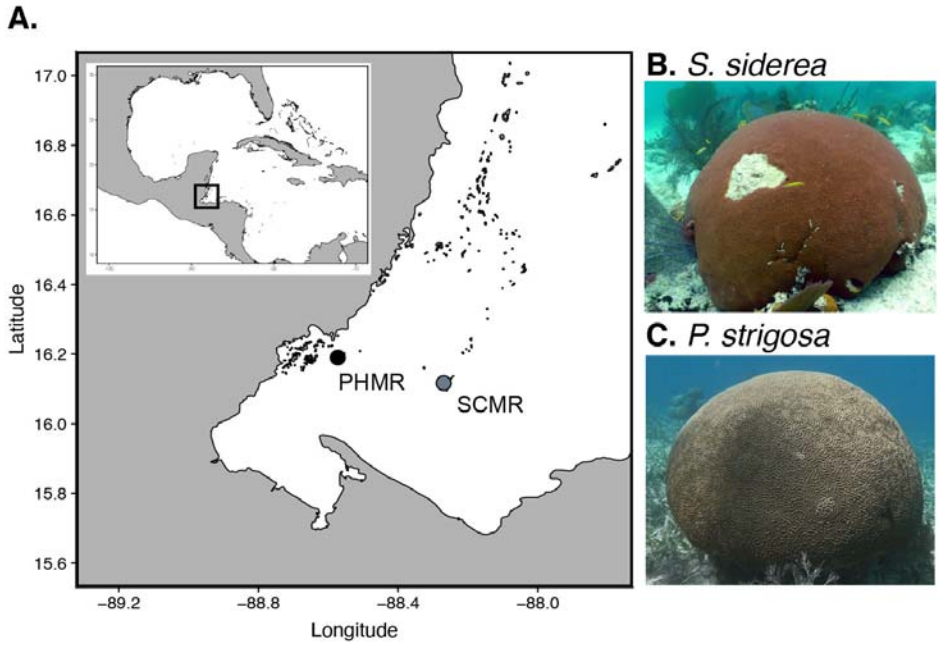

Figure 1. (A) Map of coral colony collection sites from the forereef (SCMR = Sapodilla Cayes Marine Reserve) and nearshore (PHMR = Port Honduras Marine Reserve) sites of the Belize Mesoamerican Barrier Reef System (MBRS). **(B)** Example of *Siderastrea siderea* colony (photo credit: K.D. Castillo). **(C)** Example of *Pseudodiploria strigosa* colony (photo credit: H.E. Aichelman).

Coral fragments were maintained in treatment conditions for a total of 95 days (9 August 2015 – 12 November 2015). Average (±SE) pCO_2 and temperature conditions throughout the experimental period were: 358 (±131) µatm, 28.2 (±0.1) °C; 424 (±40) µatm, 31.3 (±0.1) °C; 674 (±21) µatm, 28.0 (±0.1) °C; 606 (±36) µatm, 30.9 (±0.1) °C; 2750 (±161) µatm, 28.4

(±0.1) °C; 2917 (±174) µatm, 31.1 (±0.1) °C. Seawater parameters (including temperature, pCO_2, salinity) at each time point are shown in Figure S1 and all measured and calculated seawater parameters are reported in Tables S1 and S2, respectively.

Approximately every 30 days (exposure duration: T_0-T_{30} days = short-term, T_{30}-T_{60} days = moderate-term, T_{60}-T_{95} days = long-term), a fragment of each coral colony was removed from each of the six experimental conditions, flash frozen in liquid nitrogen, and stored at −80°C for subsequent analysis aimed at tracking genet-level physiology through time. In the event of mortality that yielded insufficient coral fragments for sampling at all time points, corals were preferentially sampled at the end of the experiment (long-term exposure: T_{95}) instead of after moderate-term exposure (T_{60}). As a result, sample sizes are lower for both species at T_{60} compared to the other time points. Following completion of the experiment, all remaining coral fragments were flash frozen in liquid nitrogen and maintained at −80°C until subsequent processing, at which time fragments were airbrushed to remove host tissue and symbiont cells. Tissue slurries were homogenized using a Tissue-Tearor (Dremel; Racine, WI, USA) and centrifuged to pelletize the symbiont cells. Coral host tissue and symbiont fractions were separated for subsequent physiological assays.

(2.2) Coral host physiology measurements

Coral growth rates were estimated over the course of the experiment using the buoyant weight technique (Davies, 1989). Buoyant weight measurements were obtained in triplicate for each coral fragment at each of the four time points (T_0, T_{30}, T_{60}, T_{95}), averaged, and normalized to the coral specimens' surface area (see methods below). As in Bove et al. (2019), a subset of fragments from both species were used to confirm the relationship between buoyant weight and dry weight. These two measurements were correlated for both species (*S. siderea* $R^2 = 0.90$, $p <$

0.001; *P. strigosa* $R^2 = 0.81$, $p < 0.001$), indicating that change in buoyant weight should reflect a proportionate change in dry weight. Equations used to calculate dry weight from buoyant weight are shown below. Dry weight was converted from g to mg, corrected to surface area of each fragment and to number of days in experimental treatment to calculate calcification rate (mg cm^{-2} day^{-1}).

S. siderea: Dry weight (g) = 1.95 * BW (g) + 3.60, $R^2 = 0.90$

P. strigosa: Dry weight (g) = 1.63 * BW (g) + 6.96, $R^2 = 0.81$

Growing surface area was quantified in triplicate from observed live tissue in photos of coral fragments taken at each timepoint using ImageJ software (Rueden et al., 2017). The same surface area values of each coral fragment were used to normalize all host and symbiont physiology parameters within an experimental timepoint.

Because corals were frozen on the same day for each time point, there was no need to correct for number of days in experimental treatment for physiological metrics other than calcification rate. Total coral host protein content was quantified from host tissue slurry using a bicinchoninic acid (BCA) protein assay. Host tissue slurry was vortexed with glass beads for 15 minutes and then centrifuged for 3 minutes at 4000 RPM. Next, 15 µL of the centrifuged sample was added to 235 µL artificial seawater along with 250 µL of Bradford reagent. After samples were mixed, absorbance was measured in a BioSpectrometer (Eppendorf, Hauppauge, NY, USA) at 562 nm. Coral protein concentrations were calculated using a standard curve of bovine serum albumin ranging from 0 to 1000 µg mL^{-1} and normalized to living coral surface area.

Total host carbohydrates were quantified using the phenol-sulfuric acid method (as in Masuko et al., 2005), which measures all monosaccharides, including glucose—the major photosynthate translocated from symbiont to coral host (Burriesci et al., 2012). An aliquot of

248 coral host tissue was diluted to 50 µL with artificial seawater (Instant Ocean Sea Salt), to which
249 150 µL of sulfuric acid and 30 µL of 5% phenol were added. Following a 5-minute incubation at
250 90°C and another 5-minute incubation at room temperature, absorbance at 490 nm was measured
251 in a spectrophotometer (Synergy H1 Microplate Reader; BioTek Instruments; VT, USA).
252 Carbohydrate concentrations were calculated using a standard curve of D-glucose solutions
253 ranging from 0.039 to 2 mg mL^{-1} and normalized to living coral surface area.

254 (2.3) Symbiodiniaceae physiology measurements

255 Symbiont cells were quantified using the hemocytometer method similar to Rodrigues
256 and Grottoli (2007). After vortexing the symbiont pellet, a 1:1 Lugol's iodine and formalin
257 solution was added for contrast and cell preservation. Triplicate 10 µL subsamples were counted
258 on a hemocytometer using a light microscope, averaged, and normalized to slurry volume and
259 live coral tissue surface area.

260 Symbiont photosynthetic pigments (chlorophyll *a*, abbreviated Chl *a*) were quantified
261 spectrophotometrically following the method of Marchetti et al. (2012). Briefly, 40 mL of 90%
262 acetone was added to the symbiont pellet, homogenized, then stored in the dark for 24 hours. 100
263 µL of each sample was then diluted in 7.9 mL of 90% acetone. A 10AU Field and Laboratory
264 Fluorometer (Turner Designs, San Jose, CA) was used to measure the initial concentration (R_b),
265 then 2 drops of 10% HCl was added to the sample tube, after which a second fluorometer reading
266 was taken (R_a). Total Chl *a* content (µg L^{-1}) was calculated using the equation below, where
267 0.548 is a calibration constant specific to the fluorometer used, 40 mL is the volume of acetone
268 left overnight, and 80 is the dilution factor. Total Chl *a* was then normalized to live coral surface
269 area to get units of µg Chl *a* cm^{-2}.

$$\text{Chl } a \left(\text{ug L}^{-1}\right) = 0.548 \times (R_b - R_a) \times 40\text{mL} \times 80$$

(2.4) Statistical analyses

All statistical analyses were completed using R version 3.5.2 (R Core Team, 2017). A series of linear models (package *lmer*) were fitted for each species and each individual physiology parameter using a forward model selection method. The best fit model was derived by starting with the intercept-only model and then using forward-selection to incorporate additional parameters, starting with the most significant parameter, until further addition of parameters did not significantly improve the model fit. Additional parameters were retained in the model if they were significant ($p < 0.05$) and produced smaller AIC values (Akaike, 1974). These parameters included fixed effects of time, temperature, pCO_2, and reef zone, which were all coded as factors. Parameter interactions were only considered if those two parameters were already significant and included in the model. A random effect of genotype was included in all models to account for physiological variation across genotypes. Note that for calcification rate data, multiple fragments of each genotype were represented at each time point. Because genotype is included in the model as a random effect, multiple fragment numbers do not artificially increase the sample size and instead only increase the precision of the rate measurement for that colony. The linear models used for each individual physiology parameter are included along with summary statistics for *S. siderea* and *P. strigosa* in Table S3. Post-hoc pairwise comparisons of significant main effects were assessed using a Tukey's HSD test, implemented in the *lsmeans* function with the option "adjust = tukey". Summary statistics for all post-hoc comparisons are reported in Table S4.

A Principal Components Analysis (PCA) was constructed using the *FactoMineR* package (Lê et al., 2008) to assess how overall physiologies were modulated through time for each species. All physiology parameters were log-transformed, and calcification rates were x+2 log-

293 transformed. Only individual coral fragments for which all physiology parameters were present
294 (calcification rate, total protein, total carbohydrate, symbiont density, Chl *a*) were included in
295 this analysis. Significance of each factor in the PCA was assessed using the *adonis()* function in
296 the *vegan* package (Oksanen, 2011), which was run with 10,000 permutations using the model
297 below. Summary statistics for all *Adonis* tests are reported in Table S5.

298 $$\text{Adonis(scores} \sim \text{reef zone} * pCO_2 * \text{temperature} + \text{genotype)}$$

299 Correlation matrices of all host and symbiont physiology parameters for both species
300 through time were built using the *corrplot()* function with a significance threshold of $p = 0.05$.
301 The impacts of temperature and pCO_2 on all host and symbiont physiology parameters of only *P.*
302 *strigosa* were assessed via linear regression modeling, as no noteworthy correlations were found
303 for *S. siderea*. To estimate significance of the predictors and their interactions, increasingly
304 parsimonious, nested linear models (using *lmer()*) were compared with likelihood ratio tests.
305 Conditional R-squared values (accounting for both fixed and random effects) of the regressions
306 were determined using the *r.squaredGLMM()* function in the *MuMIn* package. Summary
307 statistics for all linear regressions are reported in Table S6.
308 All data and code used for the analyses presented herein can be found on the GitHub
309 repository associated with this publication
310 (https://github.com/hannahaichelman/TimeCourse_Physiology).
311
312 **3. Results**
313 (3.1) Effects of thermal and acidification stress on *S. siderea* and *P. strigosa* calcification rates
314 Experiment duration ($p < 0.001$), pCO_2 ($p < 0.001$), and the interaction of experiment
315 duration and pCO_2 ($p = 0.007$), significantly influenced calcification rates of *S. siderea* (Figure

316 2A). Under extreme pCO_2 conditions, *S. siderea* calcification rates were significantly reduced
317 relative to both present day (Tukey $p < 0.001$) and next century (Tukey $p = 0.017$) pCO_2
318 treatments. Through time, calcification rates of *S. siderea* in extreme pCO_2 conditions declined
319 between T_{30} and T_{60} (Tukey $p < 0.001$), and also over the entire duration of the experiment (T_{30}
320 to T_{95}; Tukey $p < 0.001$). Temperature was not included in the best-fit model, and therefore did
321 not have a significant effect on *S. siderea* calcification.

322 *P. strigosa* calcification rates were significantly affected by experiment duration ($p <$
323 0.001), pCO_2 ($p < 0.001$), temperature ($p < 0.001$) and reef zone ($p = 0.036$) (Figure 2B).
324 Calcification rates were reduced at elevated temperature (31°C) relative to control temperature
325 (Tukey $p < 0.001$) and nearshore corals calcified faster than forereef corals (Tukey $p = 0.039$).
326 When compared to the present day pCO_2 treatment, calcification rates were also reduced under
327 extreme (Tukey $p < 0.001$) and next century pCO_2 conditions (Tukey $p = 0.017$). A significant
328 interaction of temperature and experimental duration was also detected for *P. strigosa*
329 calcification rates ($p < 0.001$), with *P. strigosa* calcification rates decreasing between T_{30} and T_{60}
330 under both control and elevated temperatures (Tukey $p < 0.05$); however, these reductions were
331 no longer detectable after moderate- and long-term exposure (T_{60} and T_{95}). When considering the
332 full duration of the experiment (T_0 to T_{95}), *P. strigosa* calcification rates decreased under
333 elevated temperature, but not under control temperature (Figure 2B). Additionally, a significant
334 interaction between reef zone and temperature on *P. strigosa* calcification rate was detected ($p =$
335 0.031), with elevated temperatures more negatively influencing calcification of forereef corals
336 than nearshore corals (Tukey $p = 0.024$). Lastly, the interaction between temperature and pCO_2
337 significantly affected *P. strigosa* calcification rates ($p = 0.0009$). There were no significant
338 differences in *P. strigosa* calcification rates amongst pCO_2 treatments under elevated

339 temperature treatments; however, calcification rates in control temperatures were significantly
340 reduced under extreme pCO_2 compared to the present day pCO_2 conditions (Tukey $p < 0.001$).

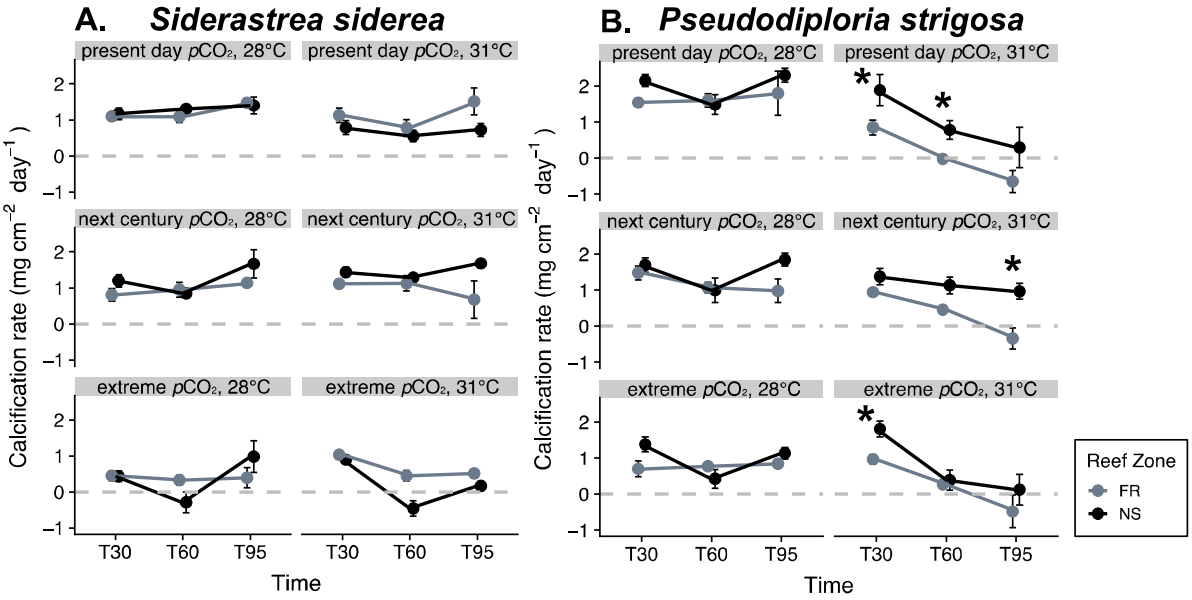

341

342 **Figure 2.** *Siderastrea siderea* **(A)** and *Pseudodiploria strigosa* **(B)** calcification rate (mg cm^{-2}
343 day^{-1}) at each experimental time point (short-term = T_{30}; moderate-term = T_{60}; long-term = T_{95}).
344 Facets represent each of the six treatments (pCO_2: present day [~400 µatm], next century [~640
345 µatm], extreme [~2800 µatm]; temperature: 28°C, 31°C) and, within a facet, data are separated
346 by reef zone ("FR" = forereef; "NS" = nearshore). Points represent mean calcification rates since
347 the previous time point (i.e. T_{30} represents calcification between T_0 and T_{30}). Asterisks (*)
348 indicate significant (Tukey $p < 0.05$) differences in calcification rates between reef zones within
349 a time point. Error bars represent standard error. For *S. siderea* (A), each data point represents
350 three colonies. For *P. strigosa* (B), each forereef point represents 2 colonies and each nearshore
351 point represents 3 colonies, except at the extreme pCO_2/28°C treatment at T_{60} and T_{95}, where
352 only one forereef colony is represented due to mortality.
353
354
355 (3.2) Effects of thermal and acidification stress on *S. siderea* and *P. strigosa* host energy reserves

356 (3.2.1) *Siderastrea siderea* total protein and total carbohydrates

357 Both experiment duration ($p < 0.001$) and temperature ($p < 0.01$) had significant effects
358 on *S. siderea* total protein content (Figure 3A), with elevated temperatures reducing total protein
359 concentrations relative to corals in control temperatures (Tukey $p = 0.01$). Regardless of pCO_2

and temperature treatments, *S. siderea* total protein content increased through time, with T_{95} exhibiting higher mean protein concentrations than T_0 (Tukey $p = 0.03$). Temperature was the only factor that influenced total carbohydrates of *S. siderea* (Figure 3C; $p < 0.01$), with significantly less carbohydrate at elevated temperature relative to the control temperature treatment (Tukey $p = 0.003$).

(3.2.2) *Pseudodiploria strigosa* total protein and total carbohydrates

For *P. strigosa*, temperature was the only factor that significantly influenced total host protein ($p < 0.001$), with reduced protein concentrations under elevated temperatures compared to control temperature treatments (Tukey $p < 0.001$). However, total carbohydrate concentrations were significantly affected by experiment duration ($p < 0.001$) and temperature ($p < 0.001$). Similar to total protein, *P. strigosa* total carbohydrate was reduced under elevated temperatures compared to control conditions (Tukey $p < 0.001$). Additionally, the interaction between experimental duration and temperature had a significant effect on *P. strigosa* carbohydrates ($p = 0.002$), with *P. strigosa* exhibiting increasing carbohydrate concentrations between T_{30} and T_{95} under control temperatures (Tukey $p = 0.004$). In contrast, under elevated temperatures, *P. strigosa* exhibited no change in carbohydrate concentrations over time (all Tukey $p > 0.05$), although a trend of decreasing carbohydrate concentrations was observed from T_0 to T_{95} (Figure 3D).

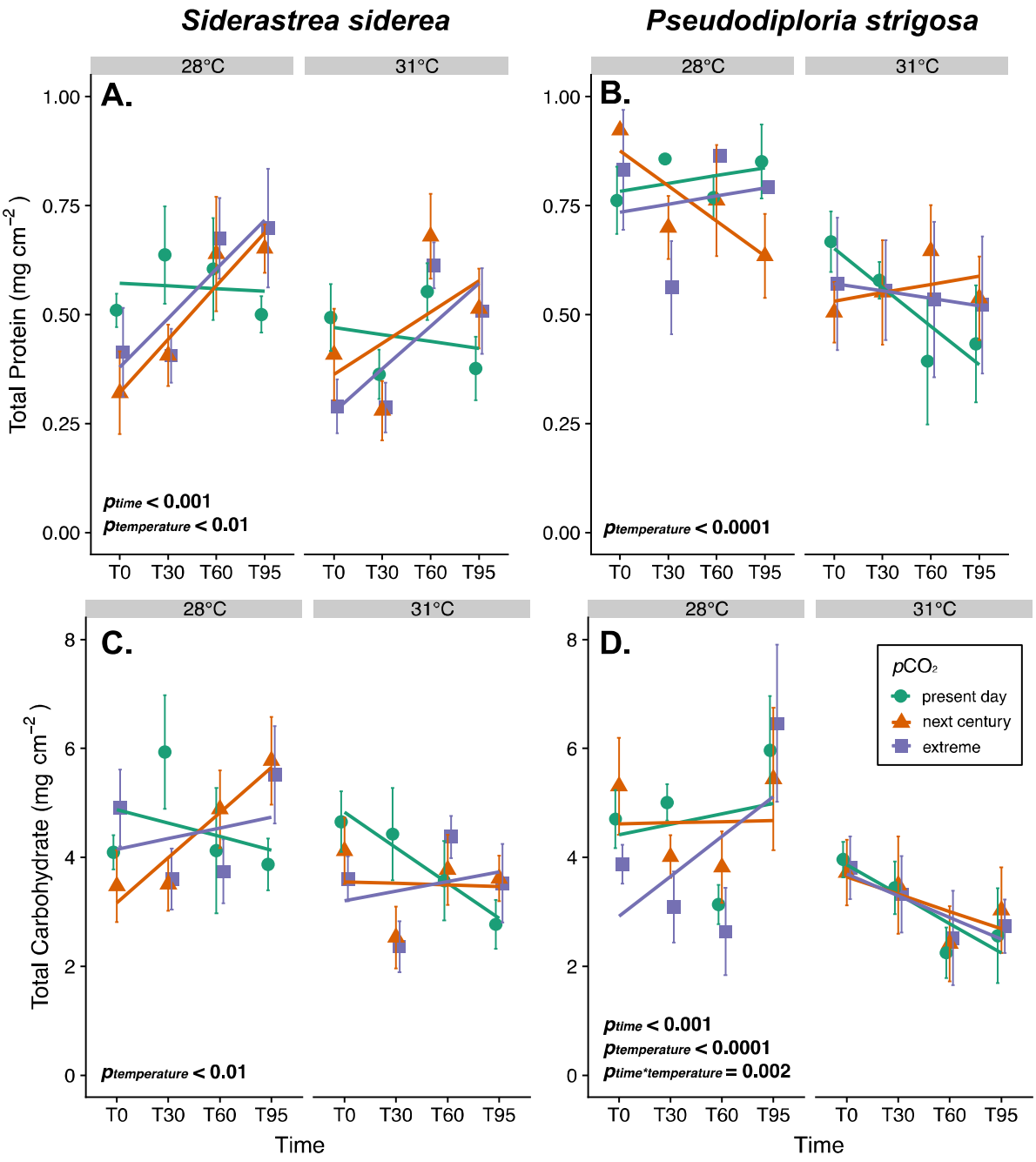

Figure 3. Host energy reserves (total protein **[A,B]** and total carbohydrate **[C,D]**) of *Siderastrea siderea* **(A,C)** and *Pseudodiploria strigosa* **(B,D)** across four experimental durations (day 0 = T_0; day 30 [short-term] = T_{30}; day 60 [moderate-term] = T_{60}; day 95 [long-term] = T_{95}). Within each panel, results are faceted by temperature treatment (28, 31°C) and colored by pCO_2 treatment (present day [~400 µatm] = green, next century [~640 µatm] = orange, extreme [~2800 µatm] = purple). Each point is an average of corals from nearshore and forereef reef zones with n = 4-6 (*S. siderea*) and n = 3-6 (*P. strigosa*) distinct fragments (n = 1 / genotype). Significant factors are indicated in each panel. Lines represent linear fits (using ggplot2 *stat_smooth()* method to

visualize differences regardless of model) for each treatment through time, and error bars represent standard error at each time point.

(3.3) Effects of thermal and acidification stress on symbiont physiology of *S. siderea* and *P. strigosa*

(3.3.1) Symbiont physiology of *S. siderea* (Chl *a* concentration, symbiont cell density)

Experiment duration ($p < 0.001$), temperature ($p < 0.01$), and pCO_2 ($p = 0.04$) had significant effects on *S. siderea* symbiont cell density (Figure 4A), with cell densities decreasing from T_0 to T_{95} (Tukey $p < 0.001$). Additionally, *S. siderea* cell densities were reduced under elevated temperatures compared to control conditions (Tukey $p = 0.017$) and under extreme pCO_2 compared to present day conditions (Tukey $p = 0.043$). The interaction between experiment duration and pCO_2 also affected *S. siderea* symbiont cell density ($p = 0.005$); however, within pCO_2 treatments the only significant change in cell densities was a decrease at low pCO_2 between T_{30} and T_{95} (Tukey $p = 0.003$). Both experiment duration ($p < 0.001$) and pCO_2 ($p < 0.001$) had significant effects on *S. siderea* Chl *a* concentration (Figure 4C). In contrast to symbiont cell density, Chl *a* concentration increased from T_0 to T_{95} (Tukey $p < 0.001$). Although corals under present day and next century pCO_2 treatments exhibited similar Chl *a* concentrations, corals under extreme pCO_2 had significantly less Chl *a* compared to those under both present day (Tukey $p = 0.002$) and next century (Tukey $p = 0.01$) pCO_2 conditions.

(3.3.2) Symbiont physiology of *P. strigosa* (Chl *a* concentration and symbiont cell density)

Experiment duration ($p < 0.001$) and temperature ($p < 0.001$) both had significant effects on *P. strigosa* symbiont cell density. Regardless of pCO_2 treatment, *P. strigosa* under elevated temperatures had reduced symbiont densities compared to corals in control temperatures (Tukey $p < 0.001$). Additionally, *P. strigosa* symbiont density was reduced at T_{95} relative to T_0 (Tukey p

412 < 0.001). Temperature ($p < 0.001$) and pCO_2 treatments ($p = 0.028$) had significant effects on *P.*
413 *strigosa* Chl *a* concentration; however, experimental duration did not. Similar to symbiont
414 density, *P. strigosa* exhibited reduced Chl *a* concentrations under elevated temperatures
415 compared to control temperatures, regardless of pCO_2 treatment (Tukey $p < 0.001$). Additionally,
416 *P. strigosa* Chl *a* concentrations were reduced under extreme pCO_2 compared to present day
417 pCO_2 treatment regardless of temperature treatment (Tukey $p = 0.02$).
418

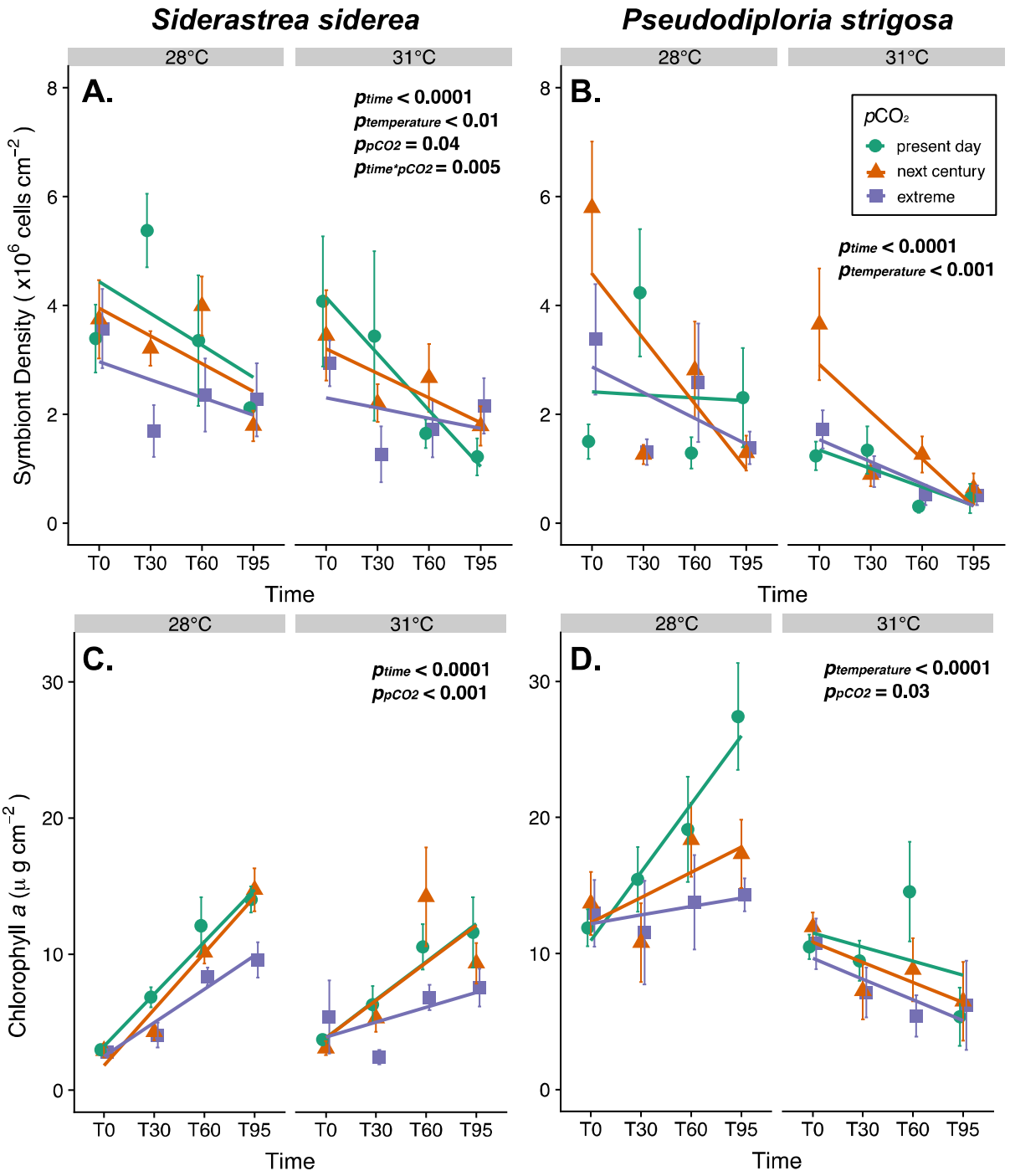

Figure 4. Symbiodiniaceae physiology (symbiont cell density **[A,B]** and Chl *a* concentration **[C,D]**) of *Siderastrea siderea* (**A,C**) and *Pseudodiploria strigosa* **(B,D)** across four experimental durations (day 0 = T_0; day 30 [short-term] = T_{30}; day 60 [moderate-term] = T_{60}; day 95 [long-term] = T_{95}). Within each panel, results are faceted by temperature treatment (28°C and 31°C) and colored by pCO_2 treatment (present day [~400 µatm] = green, next century [~640 µatm] =

orange, extreme [~2800 µatm] = purple). Points represent averages of n = 4-6 (*S. siderea*) and n = 3-6 (*P. strigosa*) fragments from nearshore and forereef reef zones (n = 1 / genotype). Significant factors are indicated in each panel. Lines represent linear fits (using ggplot2's *stat_smooth()* method to visualize differences regardless of model) for each treatment through time, and error bars are standard error at each time point.

(3.3) Holobiont physiology through time

(3.3.1) *Siderastrea siderea* holobiont physiology

Overall *S. siderea* holobiont physiology clustered more strongly by pCO_2 than by temperature (Figure 5A-C). There was a nearly significant effect of pCO_2 on holobiont physiology after short-term exposure ($T_{30,}$ Adonis p = 0.054; Figure 5A), and a significant effect at T_{95} (long-term: Adonis p = 0.002; Figure 5C). At T_{95}, the interaction of pCO_2 and temperature was also significant (Adonis p = 0.001; Figure 5C). Comparing PCAs in Figure 5A-C with individual physiology results (Figures 3A,C and 4A,C) shows that pCO_2 significantly reduced *S. siderea* calcification, symbiont density, and Chl *a* concentration, but did not have a significant effect on total carbohydrates or protein. These results are consistent with the PCA loadings for calcification, symbiont density, and Chl *a* concentration discriminating between clusters of fragments in extreme pCO_2 treatment and the other acidification treatments (Figure 5A-C). Reef zone did not have a significant main or interactive effect on *S. siderea* holobiont physiology for any exposure duration.

(3.3.2) *Pseudodiploria strigosa* holobiont physiology

Holobiont physiology of *P. strigosa* clustered more strongly by temperature than by pCO_2 treatment, especially after long-term exposure (T_{95}; Figure 5D-F). At T_{60} (moderate-term), there was a significant effect of pCO_2 on holobiont physiology (Adonis p = 0.029; Figure 5E). However, at T_{95} (long-term) the effect of pCO_2 was no longer significant, and only temperature

had a significant effect (Adonis p = 0.045; Figure 5F). Additionally, the interaction of reef zone and temperature had a marginally significant effect on holobiont physiology after long-term exposure (T_{95}; Adonis p = 0.053; Figure 5F). Comparing PCAs in Figure 5D-F with results from individual physiology parameters (Figures 3B,D and 4B,D) shows that elevated temperature had consistent negative effects on all physiology parameters.

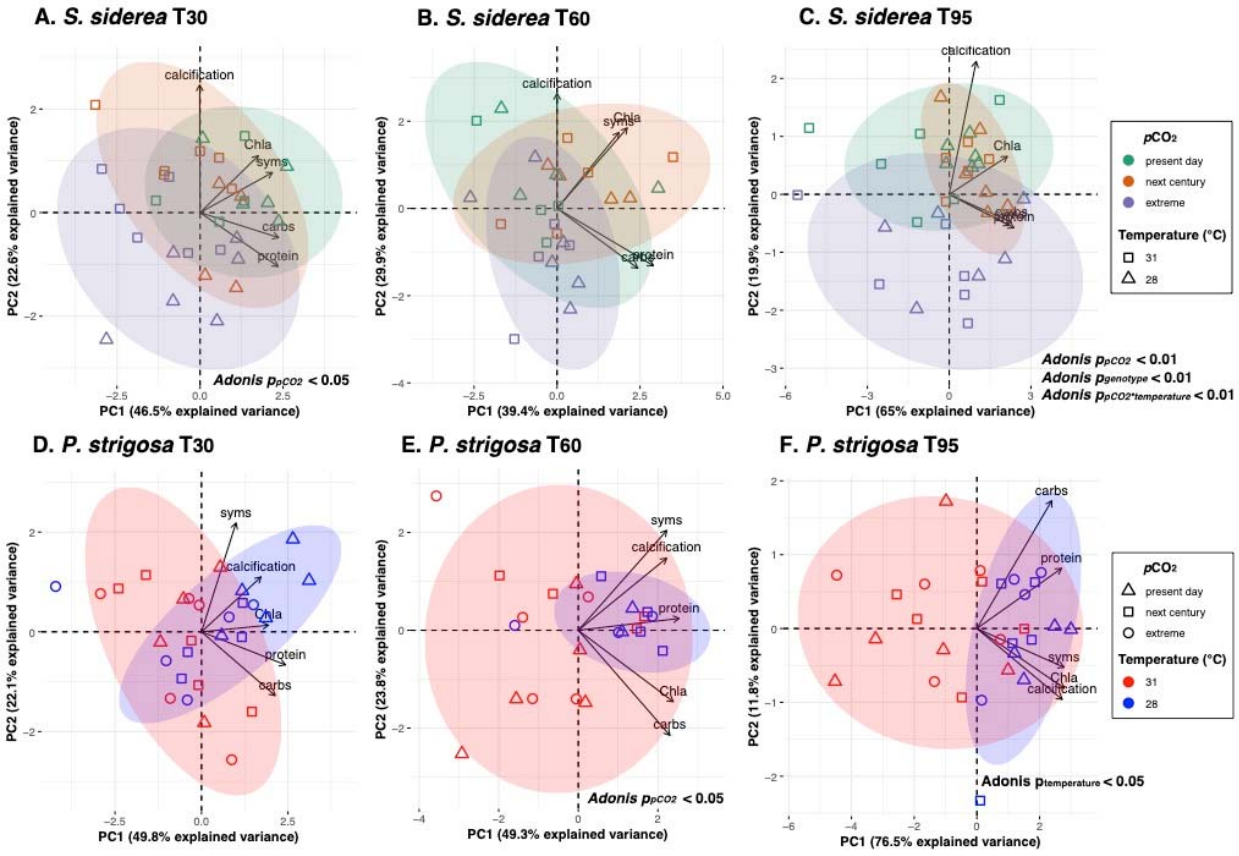

Figure 5. Influence of global change stressors and exposure duration on holobiont physiology. Principal Components Analysis (PCA) of log-transformed holobiont physiology data, including total carbohydrate (carbs; mg cm^{-2}), total protein (protein; mg cm^{-2}), symbiont density (syms; cells cm^{-2}), chlorophyll *a* concentration (Chla; ug cm^{-2}), and calcification rate (mg cm^{-2} day^{-1}) for *Siderastrea siderea* **(A-C)** and *Pseudodiploria strigosa* **(D-F)**. Colors represent pCO_2 treatment for *S. siderea* (**A-C**: green = present day [~400 µatm], orange = next century [~640 µatm], purple = extreme [~2800 µatm]) and temperature treatment for *P. strigosa* (**D-F**: red = 31°C, blue = 28°C). Shapes represent temperature treatment for *S. siderea* (**A-C**: square = 31°C, triangle = 28°C) and pCO_2 treatment for *P. strigosa* (**D-F**: triangle = present day [~400 µatm], square = next century [~640 µatm], circle = extreme [~2800 µatm]). Points represent an

individual coral fragment's combined physiology at each time point (**A,D** = short-term [T_{30}], **B,E** = moderate-term [T_{60}], **C,F** = long-term [T_{95}]). Individuals were only included if they had data for each of the five parameters at each time point. The x- and y-axes indicate the variance explained (%) by the first and second principle component, respectively.

(3.3.3) Combined species holobiont physiology

Siderastrea siderea and *P. strigosa* had distinct holobiont physiologies at all experimental durations (Adonis $p_{species} < 0.001$ for short-term [T_{30}], moderate-term [T_{60}], and long-term [T_{95}]; Figure S2; Table S5). Although species had a significant main effect on combined physiology through time, *S. siderea* and *P. strigosa* exhibit the most divergent physiologies at T_{30}, and then converge to be entirely overlapping at T_{60} and T_{95} (Figure S2). There were also significant independent effects of temperature and pCO_2 on the combined physiology for both species at each time point (Adonis $p < 0.05$ for all time points; Figure S2, Table S5).

(3.4) *Pseudodiploria strigosa* trait correlations

Pseudodiploria strigosa correlation matrices (Figure S3) revealed that calcification rate was significantly correlated with all other physiology parameters ($p < 0.05$) after 95 days of experimental treatment (long-term; T_{95}). As illustrated in *P. strigosa* results above, temperature had a main effect on the relationship between calcification and all other predictor variables (total carbohydrate and protein, symbiont density, and Chl *a* concentration; Figure 6). Correlations with calcification rate were significantly different across temperature treatment for total protein ($p = 0.04$) and symbiont density ($p = 0.001$) in *P. strigosa* at T_{95} (long-term exposure). Under elevated temperatures at T_{95}, *P. strigosa* fragments with higher total protein ($p = 0.04$) and symbiont densities ($p = 0.001$) were able to maintain faster calcification rates (Figure 6 B,C). A similar trend was observed for total carbohydrates; however, this relationship was not significant

493 (p = 0.06; Figure 6A). The interactive effect of temperature and the predictor variables on *P.*
494 *strigosa* calcification rate was not significant until the final observation point of the experiment
495 (T_{95}; Figure S4). *Siderastrea siderea* correlation matrix and linear regression analyses did not
496 reveal any significant interactions with treatment.

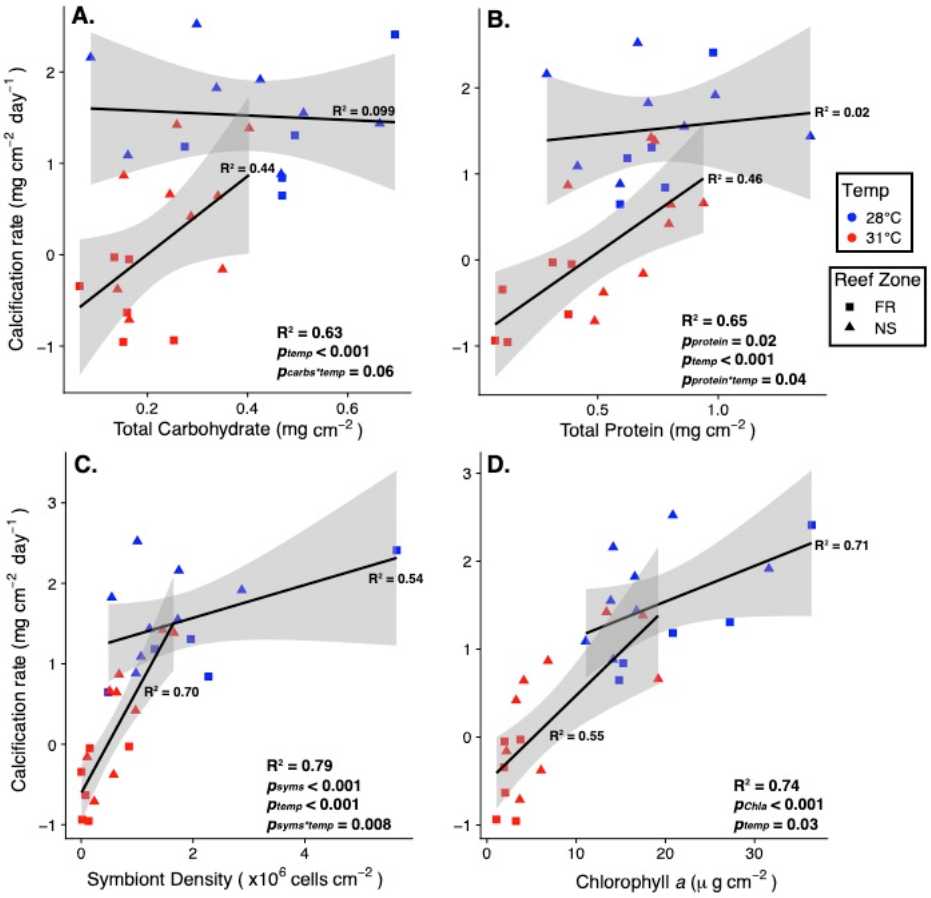

497

498 **Figure 6.** Correlations of *Pseudodiploria strigosa* calcification rate with total host carbohydrate
499 **(A),** total host protein **(B)**, symbiont density **(C)**, and chlorophyll *a* concentration **(D)** after long-
500 term exposure to experimental treatments (T_{95}). Colors represent temperature treatment (red =
501 31°C, blue = 28°C) and shapes represent reef zone (square = forereef [FR], triangle = nearshore
502 [NS]). Points represent individual coral fragments. Significant factors are indicated within each
503 panel. Lines represent linear models of measured parameters within treatment through time, fit
504 using ggplot2's *stat_smooth()* method with gray shading representing 95% confidence intervals
505 for each temperature. Conditional R-squared (R^2) values (Nakagawa and Schielzeth, 2013) are
506 reported for the whole model (bottom right corner of each facet) and for each temperature (next
507 to the line of best fit).
508

509

510

511 **4. Discussion**

512 (4.1) *Siderastrea siderea* and *P. strigosa* exhibit divergent responses to warming and
513 acidification

514 Our results demonstrate that *S. siderea* and *P. strigosa* exhibit divergent responses to two
515 co-occurring global change stressors—warming and acidification— and that these responses are
516 modulated by exposure duration (i.e. short-term = T_0-T_{30}, moderate-term = T_{30}-T_{60}, and long-
517 term = T_{60}-T_{95}). Overall physiological performance of *S. siderea* was more negatively affected
518 by acidification through time (Figure 5A-C), while temperature stress had a more negative effect
519 on *P. strigosa* physiology through time (Figure 5D-F). Such species-specific responses to
520 temperature and acidification are not uncommon in reef-building corals. For example, when
521 testing how twelve Caribbean coral species responded to crossed temperature and acidification
522 conditions for six weeks, Okazaki et al. (2017) observed some species exhibited no growth
523 response to either temperature or acidification (including *S. siderea* and *P. strigosa*), while other,
524 more abundant Florida species (e.g. *O. faveolata* and *P. astreoides*) exhibited decreased
525 calcification rates under both stressors. In contrast to Okazaki et al. (2017), we find that *S.*
526 *siderea* and *P. strigosa* holobiont physiology was significantly affected by acidification and
527 elevated temperature, respectively. Although this difference may be due to the duration of
528 experimental stress (>30 days longer than Okazaki et al. (2017)), it could also be a result of
529 Okazaki et al. (2017) using less extreme treatments (30.3°C and 1300 μatm pCO_2) than those
530 used here (31°C and 2800 μatm). It is also possible that populations of *S. siderea* and *P. strigosa*
531 in the Florida Keys, the source of corals used in the Okazaki et al. (2017) study, could be less

susceptible to stress than populations from the southern MBRS used here. According to the climate variability hypothesis (CVH; Stevens, 1989), higher latitude populations (e.g. Florida Keys) that experience more variable thermal regimes are predicted to be more phenotypically flexible and exhibit a wider range of thermal tolerances compared to populations existing closer to the equator (e.g. MBRS; Bozinovic et al., 2011). In a meta-analysis of Caribbean coral calcification responses to acidification, elevated temperature, and the combination of the two stressors, Bove et al. (2020) found similar regional differences in stress responses between corals from the Florida Keys and Belize. While calcification of Florida Keys corals did not clearly respond to acidification, elevated temperature, or their combination, elevated temperature reduced calcification rates in corals from Belize (Bove et al., 2020). While acknowledging differences in annual temperature variability, Bove et al. (2020) highlight differences in experimental treatment extremes as the main driver of calcification. While consideration of treatment level is critical, such population-level differences in stress tolerance have been previously observed in corals, for example in *Acropora millepora* across 5° of latitude on the Great Barrier Reef (Dixon et al., 2015). Regardless, results of the present study contribute to a growing body of literature supporting *S. siderea*'s resistance to conditions of elevated temperature and acidification (Banks and Foster, 2016; Bove et al., 2019; Castillo et al., 2014; Castillo et al., 2011; Davies et al., 2016).

High resistance of *S. siderea* to global change stressors was previously reported by Castillo et al. (2014), which found that only the most extreme temperature (32°C) and acidification (2553 μatm pCO_2) treatments resulted in reduced calcification rates. In the context of global change scenarios projected by the IPCC, Castillo et al. (2014) concluded that *S. siderea* will be more negatively impacted by elevated temperatures over the coming century, given that

555 the IPCC's next-century acidification projections did not reduce calcification rates. The findings
556 of the present study are consistent with this previous work, as only the extreme pCO_2 treatment–
557 but not next century pCO_2 treatment–reduced calcification rate in *S. siderea* (Figure 2A). Gene
558 expression profiling of *S. siderea* from the Castillo et al. (2014) coral fragments revealed that
559 thermal stress caused large-scale down regulation of gene expression, while acidification stress
560 elicited upregulation of proton transport genes (Davies et al., 2016), potentially offsetting the
561 effects of acidification at the site of calcification (e.g. Ries, 2011; Schoepf et al., 2017). These
562 findings provide further support for *S. siderea*'s ability to acclimate to acidification stress.

563 Bove et al. (2019) investigated the combined effects of similar temperature and
564 acidification treatments on four species of reef building corals: *S. siderea, P. strigosa, Porites*
565 *astreoides,* and *Undaria tenuifolia.* After 93 days, all species exhibited calcification declines
566 under increased pCO_2. However, *P. strigosa* was the only species that exhibited reduced
567 calcification under elevated temperature, which is consistent with results present here and
568 highlights that thermal stress more negatively impacts *P. strigosa* than *S. siderea* (Figure 5D-F).
569 Bove et al. (2019) also found that *S. siderea* was the most resistant of the four species studied, as
570 it was able to maintain positive calcification rates even in the most extreme acidification
571 treatment (~3300 μatm pCO_2)—findings that are also corroborated here (Figure 2A).
572 Interestingly, by quantifying net calcification rates at 30-day increments, we show that *S. siderea*
573 net calcification was negative under extreme pCO_2 at T_{60} and then these rates recovered by T_{95}
574 (Figure 2A). This suggests that these corals are acclimating to stressful conditions over time,
575 perhaps through transcriptome plasticity, as previously proposed by Davies et al. (2016).

576 (4.2) Stress differentially modulates coral physiology across species

Under thermal and acidification stress, corals can draw on energy reserves, including lipids, proteins, and carbohydrates, to maintain and/or produce tissue and skeleton (Anthony et al., 2009; Schoepf et al., 2013). In addition to using energetic reserves, heterotrophic feeding (Aichelman et al., 2016; Drenkard et al., 2013; Edmunds, 2011; Towle et al., 2015) or enhanced productivity of Symbiodiniaceae owing to CO_2 fertilization of symbiont photosynthesis (Brading et al., 2011) can augment energetic resources in zooxanthellate corals. Coral energetic reserves can therefore influence resistance to and recovery from stress events (Edmunds et al., 2016; Grottoli et al., 2006; Grottoli et al., 2014; Schoepf et al., 2015).

Results of the present study show that the host energy reserves (protein, carbohydrates) of *S. siderea* and *P. strigosa* responded to global change stress (warming, acidification) in different ways. Between T_0 and T_{60}, *P. strigosa* exhibited reduced carbohydrates regardless of treatment, indicating catabolism of this energy reserve (Figure 3D). This was followed by the restoration of carbohydrates (i.e. acclimation) at control temperatures at T_{95} (Figure 3D), which likely supported the positive calcification rates also observed under these conditions (Figure 6A, Figure S4). Protein reserves do not show the same trend as carbohydrates through time (Figure 3B), potentially owing to *P. strigosa* catabolizing carbohydrates before proteins, which has been observed over shorter time scales for other scleractinian coral species (Grottoli et al., 2004). However, elevated protein reserves did predict faster calcification rates in *P. strigosa* under elevated temperatures, but not until the final observation point of the experiment (T_{95}; Figure 6B, Figure S4). As photosynthate translocated from symbionts is a major source of carbohydrates to the coral host (Burriesci et al., 2012; Muscatine, 1990), reductions in symbiont cell density, Chl *a* concentration, and carbohydrates of *P. strigosa* at elevated temperature suggest that symbionts were translocating fewer resources to the host, which likely contributed to observed reductions in

calcification under these elevated temperature conditions, particularly after long-term exposure (T_{95}, Figure 6). Total protein and carbohydrate abundances of *S. siderea*, similar to those of *P. strigosa*, declined under elevated temperatures (Figure 3A,C)—consistent with previous work highlighting upregulation of protein catabolism pathways in *S. siderea* exposed to long-term thermal stress (Davies et al., 2016).

An overall trend in reduced symbiont density and increased Chl *a* concentration through time were observed under most pCO_2 and temperature conditions, except for *P. strigosa* under elevated temperature (Figure 4). Given that both species under most treatments exhibited this pattern, it cannot be ruled out that these changes in symbiont physiology were influenced by other factors, including incomplete symbiont acclimation to experimental light environment (Roth, 2014) and seasonal patterns in symbiont density and pigment concentration (Fitt et al., 2000)—which may have masked the symbiont response to thermal stress within *S. siderea*. In contrast, *P. strigosa* exhibited reduced symbiont density and Chl *a* concentrations under elevated temperature (Figure 4B,D), a pattern that is more consistent with thermally induced bleaching (Brown, 1997; Fitt et al., 2001; Glynn, 1993; Warner et al., 1999; Weis, 2008) and further illustrates the susceptibility of this species to thermal stress.

(4.3) Nearshore *P. strigosa* are more resistant than forereef conspecifics

Natal reef zone was a significant predictor of host physiology, particularly for *P. strigosa*, as nearshore corals calcified faster overall (Figure 2B). Although reef zone differences in calcification were observed for *S. siderea* (particularly through time), colonies from one reef zone did not clearly outperform colonies from the other reef zone (Figure 2A). In contrast, the reef-zone-specific calcification response of *P. strigosa* may arise from local adaptation of the host to distinct temperature regimes. On the MBRS, nearshore habitats are characterized by

623 higher maximum temperatures, greater annual temperature range, and more days above the
624 regional thermal bleaching threshold compared to forereef sites (Baumann et al., 2016). Local
625 adaptation to distinct reef zones is not uncommon in corals, and has been previously shown to
626 affect responses of corals to thermal stress. For example, *P. astreoides* was previously found to
627 be locally adapted to distinct thermal regimes in the Florida Keys, with inshore corals
628 demonstrating higher thermal tolerance, constitutively higher expression of specific metabolic
629 genes, and greater gene expression plasticity compared to offshore conspecifics (Kenkel et al.,
630 2013a; Kenkel et al., 2013b; Kenkel and Matz, 2016). Additionally, *P. strigosa* is a
631 hermaphroditic broadcast spawning species, and previous work on populations from the Flower
632 Garden Banks demonstrated that larvae have short pelagic larval durations (PLD; Davies et al.,
633 2017), which could facilitate local adaptation as larvae are more likely to locally recruit (Davies
634 et al., 2017; Mayorga-Adame et al., 2017). However, it is unknown if *P. strigosa* on the MBRS
635 have similarly short PLDs. We hypothesize that nearshore *P. strigosa* are locally adapted and/or
636 acclimated to more variable and stressful nearshore conditions, allowing maintenance of higher
637 calcification rates under thermal stress compared to their forereef counterparts.

638 It is important to note that responses to stress based on reef zone could be obscured by
639 uneven sampling across reef zones, as forereef genotypes of *P. strigosa* were slightly
640 underrepresented in the experiment (2 genotypes present vs. the standard 3) due to mortality
641 before the experiment began. It is possible that full replication of genotype would have yielded
642 different effects of reef zone in other *P. strigosa* physiology parameters.

643 Although the *S. siderea* PLD is unknown, previous work has shown high population
644 connectivity across 2,000 km of the Brazil coast (Nunes et al., 2011). If MBRS *S. siderea*
645 populations are similarly connected, it is possible that no genetic differences exist across

nearshore and forereef environments—potentially explaining the lack of reef-zone-specific responses observed here. Yet this result is inconsistent with previous findings that forereef colonies of MBRS *S. siderea* exhibited greater physiological stress than inshore colonies when exposed to higher temperatures (Castillo and Helmuth, 2005), reduced skeletal extension rates relative to inshore colonies over multi-decadal warming of the reef system (Castillo et al., 2012), and reduced symbiont photophysiology relative to inshore colonies under higher temperatures (Davies et al., 2018). However, consistent with results presented here, Bove et al. (2019) also found no evidence for reef-zone differences in physiology for *S. siderea*, or for any of the other species tested. Nevertheless, the observation that both nearshore and forereef *S. siderea* performed well under global change stressors provides further support for resistance of this species.

(4.4) Time-course experiments reveal acclimation to thermal stress in two common Caribbean corals

This study contributes to a growing body of literature demonstrating the value of assessing time-course physiology of corals exposed to global change stressors. Although studies investigating independent effects of temperature and acidification on scleractinian corals have yielded great insight into the effects of future global change on coral systems (e.g. Albright et al., 2018; Anthony et al., 2011; Carricart-Ganivet et al., 2012; Comeau et al., 2013; Jokiel and Coles, 1990; Jury et al., 2010), the combined effects of these stressors remain less explored—particularly in the context of how the coral stress response is modulated by the duration of those stressors. By characterizing coral host and symbiont physiology of a colony through time, acclimatory responses were identified in two common Caribbean reef-building coral species. The results of this study provide further evidence of the species-specific nature of this acclimation.

669 For example, under extreme pCO_2 and elevated temperature, *S. siderea* calcification rate appears
670 to recover by the end of the experiment while *P. strigosa* calcification rate declines into negative
671 net calcification. In addition to furthering our understanding of how corals could respond to
672 projected future ocean conditions, the exposure duration component of this study suggests that
673 species will exhibit differential persistence through ephemeral stress events. It is clear that local
674 heat waves that raise SST and upwelling events that reduce pH, which already threaten coral
675 populations, may threaten coral species in different ways in the future depending on the
676 timescales of these events.

677 Acclimation is an important mechanism by which corals can withstand changing
678 environmental conditions, and transcriptome plasticity is one way by which corals can acclimate
679 to stress (Davies et al., 2016; Kenkel and Matz, 2016). A coral reciprocal transplant study
680 between reef zones in the Florida Keys demonstrated that adaptive gene expression plasticity,
681 specifically plasticity of stress response genes, was associated with reduced susceptibility to a
682 summer bleaching event (Kenkel and Matz, 2016). In addition to plasticity providing a
683 mechanism for acclimation within a generation, rapid evolutionary adaptation of corals to
684 warmer oceans has also been observed on the Great Barrier Reef (Dixon et al., 2015; Matz et al.,
685 2018). However, recent widespread declines in coral abundance, diversity, and health suggest
686 that rates of intra- and trans-generational adaptation to global change stressors within most coral
687 populations are insufficient for mitigating the deleterious impacts of recent and future CO_2-
688 induced global change (Thomas et al., 2018). Understanding the interplay of acclimation and
689 adaptation in scleractinian corals is therefore essential for projecting how coral reef ecosystems
690 will fare in the higher-CO_2 future (Chevin et al., 2010; Thomas et al., 2018). This study furthers
691 understanding of how exposure duration modulates coral physiology across reef zones in two

692 prevalent Caribbean reef-building species. Future studies focusing on long-term acclimation
693 capacities of corals will further elucidate mechanisms of resistance and resilience in corals'
694 response to global stressors.
695
696
697
698
699 **5. Acknowledgements**
700 We thank the Belize Fisheries Department for all coral collection permits. Isaac Westfield,
701 Amanda Dwyer, Sara Williams, and Louise Cameron are acknowledged for assisting with
702 experimental maintenance at Northeastern University. Thanks to both the Marchetti and Septer
703 labs at the University of North Carolina at Chapel Hill (UNC) for assistance with equipment and
704 lab space to complete the physiology assays. We also thank Samir Patel, Savannah Swinea,
705 Bailey Thomasson, Forrest Buckthal, and Cori Lopazanski for assisting with preparing corals for
706 physiology assays at UNC.
707
708 **6. Funding**
709 This project was supported by NSF award OCE-1437371 (to J.B.R.), NSF award OCE-1459522
710 (to K.D.C.), NOAA award NA13OAR4310186 (to J.B.R. and K.D.C.), and the National
711 Academies of Sciences, Engineering, and Medicine Gulf Research Program Fellowship (to
712 S.W.D.). H.E.A. was supported by an NSF GRFP (2016222953) and S.W.D. was a Simons
713 Foundation Fellow of the Life Sciences Research Foundation (LSRF) while completing part of
714 this research.

7. References

Agostini, S., Fujimura, H., Higuchi, T., Yuyama, I., Casareto, B. E., Suzuki, Y. and Nakano, Y. (2013). The effects of thermal and high-CO2 stresses on the metabolism and surrounding microenvironment of the coral Galaxea fascicularis. *Comptes rendus biologies* **336**, 384-391.

Aichelman, H. E., Townsend, J. E., Courtney, T. A., Baumann, J. H., Davies, S. W. and Castillo, K. D. (2016). Heterotrophy mitigates the response of the temperate coral Oculina arbuscula to temperature stress. *Ecol. Evol* **6**, 6758-6769.

Akaike, H. (1974). A new look at the statistical model identification. *IEEE transactions on automatic control* **19**, 716-723.

Albright, R., Takeshita, Y., Koweek, D. A., Ninokawa, A., Wolfe, K., Rivlin, T., Nebuchina, Y., Young, J. and Caldeira, K. (2018). Carbon dioxide addition to coral reef waters suppresses net community calcification. *Nature* **555**, 516.

Anderson, K. D., Cantin, N. E., Casey, J. M. and Pratchett, M. S. (2019). Independent effects of ocean warming versus acidification on the growth, survivorship and physiology of two Acropora corals. *Coral Reefs* **38**, 1225-1240.

Anthony, K. R., Hoogenboom, M. O., Maynard, J. A., Grottoli, A. G. and Middlebrook, R. (2009). Energetics approach to predicting mortality risk from environmental stress: a case study of coral bleaching. *Funct Ecol* **23**, 539-550.

Anthony, K. R., Maynard, J. A., DIAZ-PULIDO, G., Mumby, P. J., Marshall, P. A., Cao, L. and HOEGH-GULDBERG, O. (2011). Ocean acidification and warming will lower coral reef resilience. *Global Change Biology* **17**, 1798-1808.

Banks, S. and Foster, K. (2016). Baseline levels of Siderastrea siderea bleaching under normal environmental conditions in Little Cayman. *Open Journal of Marine Science* **7**, 142-154.

Baumann, J. H., Townsend, J. E., Courtney, T. A., Aichelman, H. E., Davies, S. W., Lima, F. P. and Castillo, K. D. (2016). Temperature regimes impact coral assemblages along environmental gradients on lagoonal reefs in Belize. *PloS one* **11**, e0162098.

Bay, R. A. and Palumbi, S. R. (2014). Multilocus adaptation associated with heat resistance in reef-building corals. *Curr Biol* **24**, 2952-2956.

Bove, C., Umbanhowar, J. and Castillo, K. D. (2020). Meta-analysis reveals reduced coral calcification under projected ocean warming but not under acidification across the Caribbean Sea. *Frontiers in Marine Science* **7**, 127.

Bove, C. B., Ries, J. B., Davies, S. W., Westfield, I. T., Umbanhowar, J. and Castillo, K. D. (2019). Common Caribbean corals exhibit highly variable responses to future acidification and warming. *Proceedings of the Royal Society B* **286**, 20182840.

Bozinovic, F., Calosi, P. and Spicer, J. I. (2011). Physiological correlates of geographic range in animals. *Annu. Rev. Ecol. Evol. Syst.* **42**, 155-179.

Brading, P., Warner, M. E., Davey, P., Smith, D. J., Achterberg, E. P. and Suggett, D. J. (2011). Differential effects of ocean acidification on growth and photosynthesis among phylotypes of Symbiodinium (Dinophyceae). *Limnol Oceanogr* **56**, 927-938.

Brown, B. E. (1997). Coral bleaching: causes and consequences. *Coral reefs* **16**, S129-S138.

Burriesci, M. S., Raab, T. K. and Pringle, J. R. (2012). Evidence that glucose is the major transferred metabolite in dinoflagellate–cnidarian symbiosis. *J. Exp. Biol.* **215**, 3467-3477.

Carricart-Ganivet, J. P., Cabanillas-Teran, N., Cruz-Ortega, I. and Blanchon, P. (2012). Sensitivity of calcification to thermal stress varies among genera of massive reef-building corals. *PLoS One* **7**, e32859.

Castillo, K. and Helmuth, B. (2005). Influence of thermal history on the response of *Montastraea annularis* to short-term temperature exposure. *Mar. Biol* **148**, 261-270.

Castillo, K. D., Ries, J. B., Bruno, J. F. and Westfield, I. T. (2014). The reef-building coral Siderastrea siderea exhibits parabolic responses to ocean acidification and warming. *Proceedings of the Royal Society of London B: Biological Sciences* **281**, 20141856.

Castillo, K. D., Ries, J. B. and Weiss, J. M. (2011). Declining coral skeletal extension for forereef colonies of Siderastrea siderea on the Mesoamerican Barrier Reef System, Southern Belize. *PLoS One* **6**.

Castillo, K. D., Ries, J. B., Weiss, J. M. and Lima, F. P. (2012). Decline of forereef corals in response to recent warming linked to history of thermal exposure. *Nat. Clim. Change*. **2**, 756.

Chevin, L.-M., Lande, R. and Mace, G. M. (2010). Adaptation, plasticity, and extinction in a changing environment: towards a predictive theory. *PLoS biology* **8**, e1000357.

Chua, C. M., Leggat, W., Moya, A. and Baird, A. H. (2013). Temperature affects the early life history stages of corals more than near future ocean acidification. *Mar Ecol Prog Ser.* **475**, 85-92.

Cohen, A. L. and Holcomb, M. (2009). Why corals care about ocean acidification: uncovering the mechanism. *Oceanography* **22**, 118-127.

Comeau, S., Carpenter, R. and Edmunds, P. (2013). Coral reef calcifiers buffer their response to ocean acidification using both bicarbonate and carbonate. *Proceedings of the Royal Society B: Biological Sciences* **280**, 20122374.

Comeau, S., Cornwall, C., DeCarlo, T., Doo, S., Carpenter, R. and McCulloch, M. (2019). Resistance to ocean acidification in coral reef taxa is not gained by acclimatization. *Nat. Clim. Change*. **9**, 477.

Costanza, R., de Groot, R., Sutton, P., Van der Ploeg, S., Anderson, S. J., Kubiszewski, I., Farber, S. and Turner, R. K. (2014). Changes in the global value of ecosystem services. *Global environmental change* **26**, 152-158.

Davies, P. S. (1989). Short-term growth measurements of corals using an accurate buoyant weighing technique. *Mar. Biol* **101**, 389-395.

Davies, S. W., Marchetti, A., Ries, J. B. and Castillo, K. D. (2016). Thermal and pCO2 stress elicit divergent transcriptomic responses in a resilient coral. *Frontiers in Marine Science* **3**, 112.

Davies, S. W., Ries, J. B., Marchetti, A. and Castillo, K. D. (2018). Symbiodinium functional diversity in the coral Siderastrea siderea is influenced by thermal stress and reef environment, but not ocean acidification. *Frontiers in Marine Science* **5**, 150.

Davies, S. W., Strader, M. E., Kool, J. T., Kenkel, C. D. and Matz, M. V. (2017). Modeled differences of coral life-history traits influence the refugium potential of a remote Caribbean reef. *Coral Reefs* **36**, 913-925.

Dixon, G. B., Davies, S. W., Aglyamova, G. V., Meyer, E., Bay, L. K. and Matz, M. V. (2015). Genomic determinants of coral heat tolerance across latitudes. *Science* **348**, 1460-1462.

Doney, S. C., Fabry, V. J., Feely, R. A. and Kleypas, J. A. (2009). Ocean acidification: the other CO2 problem. *Ann Rev Mar Sci.* **1**, 169-192.

Drenkard, E. J., Cohen, A. L., McCorkle, D. C., de Putron, S. J., Starczak, V. R. and Zicht, A. (2013). Calcification by juvenile corals under heterotrophy and elevated CO 2. *Coral Reefs* **32**, 727-735.

Edmunds, P. J. (2011). Zooplanktivory ameliorates the effects of ocean acidification on the reef coral Porites spp. *Limnol Oceanogr* **56**, 2402-2410.

Edmunds, P. J., Brown, D. and Moriarty, V. (2012). Interactive effects of ocean acidification and temperature on two scleractinian corals from Moorea, French Polynesia. *Global Change Biology* **18**, 2173-2183.

Edmunds, P. J., Comeau, S., Lantz, C., Andersson, A., Briggs, C., Cohen, A., Gattuso, J.-P., Grady, J. M., Gross, K. and Johnson, M. (2016). Integrating the effects of ocean acidification across functional scales on tropical coral reefs. *Bioscience* **66**, 350-362.

Edmunds, P. J., Doo, S. S. and Carpenter, R. C. (2019). Changes in coral reef community structure in response to year-long incubations under contrasting pCO 2 regimes. *Mar. Biol* **166**, 94.

Fitt, W. K., Brown, B. E., Warner, M. E. and Dunne, R. P. (2001). Coral bleaching: interpretation of thermal tolerance limits and thermal thresholds in tropical corals. *Coral Reefs* **20**, 51-65.

Fitt, W. K., McFarland, F., Warner, M. E. and Chilcoat, G. C. (2000). Seasonal patterns of tissue biomass and densities of symbiotic dinoflagellates in reef corals and relation to coral bleaching. *Limnol Oceanogr* **45**, 677-685.

Glynn, P. (1993). Coral reef bleaching: ecological perspectives. *Coral reefs* **12**, 1-17.

Grottoli, A., Rodrigues, L. and Juarez, C. (2004). Lipids and stable carbon isotopes in two species of Hawaiian corals, Porites compressa and Montipora verrucosa, following a bleaching event. *Mar. Biol* **145**, 621-631.

Grottoli, A. G., Rodrigues, L. J. and Palardy, J. E. (2006). Heterotrophic plasticity and resilience in bleached corals. *Nature* **440**, 1186.

Grottoli, A. G., Warner, M. E., Levas, S. J., Aschaffenburg, M. D., Schoepf, V., McGinley, M., Baumann, J. and Matsui, Y. (2014). The cumulative impact of annual coral bleaching can turn some coral species winners into losers. *Global Change Biology* **20**, 3823-3833.

Hoegh-Guldberg, O., Mumby, P. J., Hooten, A. J., Steneck, R. S., Greenfield, P., Gomez, E., Harvell, C. D., Sale, P. F., Edwards, A. J. and Caldeira, K. (2007). Coral reefs under rapid climate change and ocean acidification. *science* **318**, 1737-1742.

Holcomb, M., Cohen, A. L. and McCorkle, D. C. (2012). An investigation of the calcification response of the scleractinian coral *Astrangia poculata* to elevated pCO2 and the effects of nutrients, zooxanthellae and gender. *Biogeosciences* **9**, 29-39.

Horvath, K. M., Castillo, K. D., Armstrong, P., Westfield, I. T., Courtney, T. and Ries, J. B. (2016). Next-century ocean acidification and warming both reduce calcification rate, but only acidification alters skeletal morphology of reef-building coral Siderastrea siderea. *Sci Rep.* **6**, 29613.

Hughes, T. P., Kerry, J. T., Álvarez-Noriega, M., Álvarez-Romero, J. G., Anderson, K. D., Baird, A. H., Babcock, R. C., Beger, M., Bellwood, D. R. and Berkelmans, R. (2017). Global warming and recurrent mass bleaching of corals. *Nature* **543**, 373.

Jokiel, P. and Coles, S. (1990). Response of Hawaiian and other Indo-Pacific reef corals to elevated temperature. *Coral reefs* **8**, 155-162.

Jokiel, P., Rodgers, K., Kuffner, I., Andersson, A., Cox, E. and Mackenzie, F. (2008). Ocean acidification and calcifying reef organisms: a mesocosm investigation. *Coral reefs* **27**, 473-483.

Jury, C. P., Whitehead, R. F. and Szmant, A. M. (2010). Effects of variations in carbonate chemistry on the calcification rates of Madracis auretenra (= Madracis mirabilis sensu Wells, 1973): bicarbonate concentrations best predict calcification rates. *Global Change Biology* **16**, 1632-1644.

Kenkel, C., Goodbody-Gringley, G., Caillaud, D., Davies, S., Bartels, E. and Matz, M. (2013a). Evidence for a host role in thermotolerance divergence between populations of the mustard hill coral (*Porites astreoides*) from different reef environments. *Mol Ecol* **22**, 4335-4348.

Kenkel, C., Meyer, E. and Matz, M. (2013b). Gene expression under chronic heat stress in populations of the mustard hill coral (P orites astreoides) from different thermal environments. *Mol Ecol* **22**, 4322-4334.

Kenkel, C. D. and Matz, M. V. (2016). Gene expression plasticity as a mechanism of coral adaptation to a variable environment. *Nat. Ecol. Evol.* **1**, 0014.

Kleypas, J. A., Buddemeier, R. W., Archer, D., Gattuso, J.-P., Langdon, C. and Opdyke, B. N. (1999). Geochemical consequences of increased atmospheric carbon dioxide on coral reefs. *science* **284**, 118-120.

Kline, D. I., Teneva, L., Okamoto, D. K., Schneider, K., Caldeira, K., Miard, T., Chai, A., Marker, M., Dunbar, R. B. and Mitchell, B. G. (2019). Living coral tissue slows skeletal dissolution related to ocean acidification. *Nat. Ecol. Evol.* **3**, 1438-1444.

Kornder, N. A., Riegl, B. M. and Figueiredo, J. (2018). Thresholds and drivers of coral calcification responses to climate change. *Global change biology* **24**, 5084-5095.

Kroeker, K. J., Kordas, R. L., Crim, R., Hendriks, I. E., Ramajo, L., Singh, G. S., Duarte, C. M. and Gattuso, J. P. (2013). Impacts of ocean acidification on marine organisms: quantifying sensitivities and interaction with warming. *Global change biology* **19**, 1884-1896.

Kroeker, K. J., Kordas, R. L., Crim, R. N. and Singh, G. G. (2010). Meta-analysis reveals negative yet variable effects of ocean acidification on marine organisms. *Ecol Lett* **13**, 1419-1434.

LaJeunesse, T. C., Parkinson, J. E., Gabrielson, P. W., Jeong, H. J., Reimer, J. D., Voolstra, C. R. and Santos, S. R. (2018). Systematic revision of Symbiodiniaceae highlights the antiquity and diversity of coral endosymbionts. *Curr Biol* **28**, 2570-2580. e6.

Lê, S., Josse, J. and Husson, F. (2008). FactoMineR: an R package for multivariate analysis. *Journal of statistical software* **25**, 1-18.

Levas, S., Schoepf, V., Warner, M. E., Aschaffenburg, M., Baumann, J. and Grottoli, A. G. (2018). Long-term recovery of Caribbean corals from bleaching. *J. Exp. Mar. Biol. Ecol* **506**, 124-134.

Marchetti, A., Schruth, D. M., Durkin, C. A., Parker, M. S., Kodner, R. B., Berthiaume, C. T., Morales, R., Allen, A. E. and Armbrust, E. V. (2012). Comparative metatranscriptomics identifies molecular bases for the physiological responses of phytoplankton to varying iron availability. *Proceedings of the National Academy of Sciences* **109**, E317-E325.

Masuko, T., Minami, A., Iwasaki, N., Majima, T., Nishimura, S.-I. and Lee, Y. C. (2005). Carbohydrate analysis by a phenol–sulfuric acid method in microplate format. *Analytical biochemistry* **339**, 69-72.

Matz, M. V., Treml, E. A., Aglyamova, G. V. and Bay, L. K. (2018). Potential and limits for rapid genetic adaptation to warming in a Great Barrier Reef coral. *PLoS genetics* **14**, e1007220.

Mayorga-Adame, C. G., Batchelder, H. P. and Spitz, Y. (2017). Modeling larval connectivity of coral reef organisms in the Kenya-Tanzania region. *Frontiers in Marine Science* **4**, 92.

McLachlan, R. H., Price, J. T., Solomon, S. L. and Grottoli, A. G. (2020). Thirty years of coral heat-stress experiments: a review of methods. *Coral Reefs*, 1-18.

Morley, J. W., Selden, R. L., Latour, R. J., Frölicher, T. L., Seagraves, R. J. and Pinsky, M. L. (2018). Projecting shifts in thermal habitat for 686 species on the North American continental shelf. *PloS one* **13**, e0196127.

Muscatine, L. (1990). The role of symbiotic algae in carbon and energy flux in reef corals. *Ecosystems of the world. Coral Reefs*.

Nakagawa, S. and Schielzeth, H. (2013). A general and simple method for obtaining R2 from generalized linear mixed-effects models. *Methods in ecology and evolution* **4**, 133-142.

Nunes, F. L., Norris, R. D. and Knowlton, N. (2011). Long distance dispersal and connectivity in amphi-Atlantic corals at regional and basin scales. *PloS one* **6**, e22298.

Okazaki, R. R., Towle, E. K., van Hooidonk, R., Mor, C., Winter, R. N., Piggot, A. M., Cunning, R., Baker, A. C., Klaus, J. S. and Swart, P. K. (2017). Species-specific responses to climate change and community composition determine future calcification rates of Florida Keys reefs. *Global change biology* **23**, 1023-1035.

Oksanen, J. (2011). Vegan: community ecology package. R package ver. 2.0-2. *http://CRAN. R-project. org/package= vegan*.

Oliver, T. and Palumbi, S. (2011). Do fluctuating temperature environments elevate coral thermal tolerance? *Coral Reefs* **30**, 429-440.

Orr, J. C., Fabry, V. J., Aumont, O., Bopp, L., Doney, S. C., Feely, R. A., Gnanadesikan, A., Gruber, N., Ishida, A. and Joos, F. (2005). Anthropogenic ocean acidification over the twenty-first century and its impact on calcifying organisms. *Nature* **437**, 681.

Palumbi, S. R., Barshis, D. J., Traylor-Knowles, N. and Bay, R. A. (2014). Mechanisms of reef coral resistance to future climate change. *Science* **344**, 895-898.

Parmesan, C. and Yohe, G. (2003). A globally coherent fingerprint of climate change impacts across natural systems. *Nature* **421**, 37.

Pörtner, H., Roberts, D., Masson-Delmotte, V., Zhai, P., Tignor, M., Poloczanska, E., Mintenbeck, K., Nicolai, M., Okem, A. and Petzold, J. (2019). IPCC Special Report on the Ocean and Cryosphere in a Changing Climate. *IPCC Intergovernmental Panel on Climate Change: Geneva, Switzerland*.

Prada, F., Caroselli, E., Mengoli, S., Brizi, L., Fantazzini, P., Capaccioni, B., Pasquini, L., Fabricius, K., Dubinsky, Z. and Falini, G. (2017). Ocean warming and acidification synergistically increase coral mortality. *Sci Rep.* **7**, 1-10.

R Core Team. (2017). R: A language and environment for statistical computing. Vienna, Austria.

Reynaud, S., Leclercq, N., Romaine-Lioud, S., Ferrier-Pagés, C., Jaubert, J. and Gattuso, J. P. (2003). Interacting effects of CO2 partial pressure and temperature on

photosynthesis and calcification in a scleractinian coral. *Global Change Biology* **9**, 1660-1668.

Ries, J., Cohen, A. and McCorkle, D. (2010). A nonlinear calcification response to CO 2-induced ocean acidification by the coral Oculina arbuscula. *Coral Reefs* **29**, 661-674.

Ries, J. B. (2011). A physicochemical framework for interpreting the biological calcification response to CO2-induced ocean acidification. *Geochim. Cosmochim. Acta* **75**, 4053-4064.

Rodolfo-Metalpa, R., Houlbrèque, F., Tambutté, É., Boisson, F., Baggini, C., Patti, F. P., Jeffree, R., Fine, M., Foggo, A. and Gattuso, J. (2011). Coral and mollusc resistance to ocean acidification adversely affected by warming. *Nat. Clim. Change.* **1**, 308.

Rodolfo-Metalpa, R., Peirano, A., Houlbrèque, F., Abbate, M. and Ferrier-Pagès, C. (2008). Effects of temperature, light and heterotrophy on the growth rate and budding of the temperate coral Cladocora caespitosa. *Coral Reefs* **27**, 17-25.

Rodrigues, L. J. and Grottoli, A. G. (2007). Energy reserves and metabolism as indicators of coral recovery from bleaching. *Limnol Oceanogr* **52**, 1874-1882.

Roth, M. S. (2014). The engine of the reef: photobiology of the coral–algal symbiosis. *Front Microbiol.* **5**, 422.

Rueden, C. T., Schindelin, J., Hiner, M. C., DeZonia, B. E., Walter, A. E., Arena, E. T. and Eliceiri, K. W. (2017). ImageJ2: ImageJ for the next generation of scientific image data. *BMC bioinformatics* **18**, 529.

Schoepf, V., Grottoli, A. G., Levas, S. J., Aschaffenburg, M. D., Baumann, J. H., Matsui, Y. and Warner, M. E. (2015). Annual coral bleaching and the long-term recovery capacity of coral. *Proceedings of the Royal Society B: Biological Sciences* **282**, 20151887.

Schoepf, V., Grottoli, A. G., Warner, M. E., Cai, W.-J., Melman, T. F., Hoadley, K. D., Pettay, D. T., Hu, X., Li, Q. and Xu, H. (2013). Coral energy reserves and calcification in a high-CO2 world at two temperatures. *PloS one* **8**, e75049.

Schoepf, V., Jury, C. P., Toonen, R. J. and McCulloch, M. T. (2017). Coral calcification mechanisms facilitate adaptive responses to ocean acidification. *Proceedings of the Royal Society B: Biological Sciences* **284**, 20172117.

Shaw, E. C., Carpenter, R. C., Lantz, C. A. and Edmunds, P. J. (2016). Intraspecific variability in the response to ocean warming and acidification in the scleractinian coral Acropora pulchra. *Mar. Biol* **163**, 210.

Stevens, G. C. (1989). The latitudinal gradient in geographical range: how so many species coexist in the tropics. *Am. Nat.* **133**, 240-256.

Thomas, L., Rose, N. H., Bay, R. A., López, E. H., Morikawa, M. K., Ruiz-Jones, L. and Palumbi, S. R. (2018). Mechanisms of thermal tolerance in reef-building corals across a fine-grained environmental mosaic: Lessons from Ofu, American Samoa. *Frontiers in Marine Science* **4**, 434.

Towle, E. K., Enochs, I. C. and Langdon, C. (2015). Threatened Caribbean coral is able to mitigate the adverse effects of ocean acidification on calcification by increasing feeding rate. *PloS one* **10**, e0123394.

Warner, M. E., Fitt, W. K. and Schmidt, G. W. (1999). Damage to photosystem II in symbiotic dinoflagellates: a determinant of coral bleaching. *Proceedings of the National Academy of Sciences* **96**, 8007-8012.

Weis, V. M. (2008). Cellular mechanisms of Cnidarian bleaching: stress causes the collapse of symbiosis. *J. Exp. Biol.* **211**, 3059-3066.